Marine Pollution Bulletin 191 (2023) 114870

Contents lists available at ScienceDirect

Marine Pollution Bulletin

journal homepage: www.elsevier.com/locate/marpolbul

First in-situ monitoring of sponge response and recovery to an industrial sedimentation event

Jennifer M. Durden [a,*], Michael A. Clare [a], Johanne Vad [b], Andrew R. Gates [a]

[a] National Oceanography Centre, Southampton, UK
[b] University of Edinburgh, Edinburgh, UK

ARTICLE INFO

Keywords:
Environmental impact
Sediment plume
Smothering
Hydrocarbon drilling
Deep-sea mining
Drilling mud

ABSTRACT

Assessment of risks to seabed habitats from industrial activities is based on the resilience and potential for recovery. Increased sedimentation, a key impact of many offshore industries, results in burial and smothering of benthic organisms. Sponges are particularly vulnerable to increases in suspended and deposited sediment, but response and recovery have not been observed in-situ. We quantified the impact of sedimentation from offshore hydrocarbon drilling over ~5 days on a lamellate demosponge, and its recovery in-situ over ~40 days using hourly time-lapse photographs with measurements of backscatter (a proxy of suspended sediment) and current speed. Sediment accumulated on the sponge then cleared largely gradually but occasionally sharply, though it did not return to the initial state. This partial recovery likely involved a combination of active and passive removal. We discuss the use of in-situ observing, which is critical to monitoring impacts in remote habitats, and need for calibration to laboratory conditions.

1. Introduction

The sustainable development of the marine environment is predicated on understanding the impact of anthropogenic activities to evaluate risks and apply mitigations where needed. Assessments of the risks posed to seabed habitats from industrial activities, such as dredging, hydrocarbon exploration and production, and deep-sea mining (Washburn et al., 2019), is based on the resilience and potential for recovery from such activities determined from experiments and in-situ observation (Gates and Jones, 2012; Gollner et al., 2017; Jones et al., 2012; Jones et al., 2017; Roegner et al., 2021). The evaluation of risk from industrial development to the seabed ranges from project-level Environmental Impact Assessment (Durden et al., 2018) to regional environmental management plans and conservation measures (e.g., Marine Protected Areas; Wedding et al., 2013), implemented through environmental management policies. A key impact common to a wide range of offshore industries is increased sedimentation (Bradshaw et al., 2012), in which added materials and resuspended natural sediment are deposited, resulting in the smothering, burying, clogging and choking of suspension-feeding organisms (Roegner et al., 2021). Increased sedimentation results in reductions in the abundance, diversity and functioning of benthic organisms (Jones et al., 2006), with resilience and recovery varying between organism type (Gollner et al., 2017; Jones et al., 2017). Understanding how benthic organisms respond to industrial impacts, particularly species of conservation importance such as sponges, is important for robust policy development. Despite this importance, response and recovery are poorly understood in real-world conditions due to a paucity of time-referenced field-scale observations.

Sponges are important to community diversity and structure across benthic habitats in areas targeted by industry from shallow to deep water (Durden et al., 2021; Kazanidis et al., 2019; Mitchell and Harris, 2020; Vieira et al., 2020). They also provide important structural complexity to the benthic environment, which functions as habitats for other fauna, including macrofauna (Beaulieu, 2001; Bett and Rice, 1992; Laguionie-Marchais et al., 2015) and demersal fish (Kenchington et al., 2013). Sponges are also important contributors to bentho-pelagic coupling, and impact food webs and biogeochemical cycles through respiration, and organic carbon and nutrient cycling (Cathalot et al., 2015; Maldonado et al., 2012). Their importance as key benthic habitats makes sponges targets of conservation and management measures (Maldonado et al., 2015), requiring information on their response and resilience to anthropogenic activities, such as trawling (Pusceddu et al., 2014; Vieira et al., 2020) and oil and gas production (Vad et al., 2018).

As suspension feeders, sponges are particularly vulnerable to

* Corresponding author.
E-mail address: Jennifer.durden@noc.ac.uk (J.M. Durden).

https://doi.org/10.1016/j.marpolbul.2023.114870
Received 9 December 2022; Received in revised form 27 February 2023; Accepted 20 March 2023
Available online 16 April 2023
0025-326X/© 2023 The Authors. Published by Elsevier Ltd. This is an open access article under the CC BY license (http://creativecommons.org/licenses/by/4.0/).

increases in suspended and deposited sediment above background levels. Previous studies of the impacts of sedimentation on sponges have largely been short-term ex-situ laboratory experiments, and found both direct and indirect effects (reviewed by Bell et al., 2015), including changes to respiration (Bannister et al., 2012; Lohrer et al., 2006), pumping (Pineda et al., 2017; Tompkins-MacDonald and Leys, 2008), filtration and feeding (Bannister et al., 2012; Grant et al., 2018; Tjensvoll et al., 2013), reproduction and growth (Maldonado et al., 2008; Roberts et al., 2006; Whalan et al., 2007), and physiological parameters (Mobilia et al., 2021). Sponges have been observed to tolerate stress and even recover from increased sedimentation (Kutti et al., 2015), through active and passive strategies, including changes to movement behaviour (Grant et al., 2018; Strehlow et al., 2017). Both the type and magnitude of impact, and the ability to recover from sedimentation are related to the concentrations and duration of exposure (Kutti et al., 2015; Strehlow et al., 2017). However, in-situ observations are required to understand the real-world impact and recovery of sponges from sedimentation, but remain extremely rare (Bell et al., 2015).

We observe and quantify the impact of sedimentation associated with the drilling of an offshore oil well on a deep-water sponge, and its recovery in-situ using novel photographic and oceanographic data acquired during a time-lapse field study. First, we characterise the nature of a disturbance event associated with the release of drilling mud and cuttings from hydrocarbon drilling, and the influence of resuspension of natural seabed sediment by near-bed currents. Direct water column measurements provide constraint to the timing and influence of near-bed currents and allow us to link the period of increased turbidity to deposition on the sponge. Second, we monitor the in-situ response of the sponge using hourly time-lapse photographs. We monitor sediment accumulation on the sponge and its movement to build a picture of its response and any recovery. Third, we place our field results in a wider context, to compare with prior, largely laboratory-based, experimental studies to identify the possible mechanisms for sponge recovery. Finally, we discuss opportunities and guidance for future field monitoring that is required to better characterise the diverse range of acute and chronic impacts posed to sponges and other suspension feeders by the growing human use of the seabed.

2. Methods

2.1. Field operations

Field operations were conducted from the Transocean Leader semi-submersible drill rig in the vicinity of the site of a new Hurricane Energy well in the Warwick Crestal block on the on the slope west of Shetland (Warwick Crestal 204/30b-A; 60° 07′ 25.476″ N, 004° 09′ 28.836″ W; 156 m water depth; Gates and Durden, 2021). The Faroe Shetland Channel and slope west of Shetland have been the site of oil and gas exploration and production for decades.

The seabed morphology in the area is characterised by iceberg ploughmarks (formed during previous glacial episodes) and stony reef habitats on cobbles and boulders (Bett, 2012). OSPAR Commission (2010) notes the potential for deep-sea sponge aggregations in the area associated with these two features. The environmental baseline assessment of the well site found the seabed to consist of linear ENE/WSW bands of mixed sediments (gravelly sand, slightly gravelly sand, sand) interspersed with bands of coarser sediment (sandy gravel, larger gravel, cobbles, boulders) (GeoXYZ Benthic Solutions, 2019b), and suggested that EUNIS habitat types of 'Offshore Circalittoral Coarse Sediment' and 'Offshore Circalittoral Mixed Sediment' (GEOXYZ Benthic Solutions, 2019a). Particle size was bimodal in distribution, with peaks at very coarse sand (710 μm < x < 2 mm) and medium sand (180 μm < x < 500 μm); sediment samples at 50 m from the well location contained mean particle sizes of 0.98 and 1.14 mm (GeoXYZ Benthic Solutions, 2019b). Several types of sponges have been documented in the area, including demosponges, such as *Geodia* and *Phakellia* (Bett, 2001; Taboada et al., 2022). Two Marine Protected Areas lie in the vicinity: the Faroe-Shetland Sponge Belt MPA, and the West Shetland Shelf MPA to the south (Joint Nature Conservation Committee, 2014a; Joint Nature Conservation Committee, 2014b).

In situ observations were made over the initial period of well drilling by deploying a time-lapse camera and a current meter that also recorded acoustic backscatter (Durden and Gates, 2022). The time-lapse camera with strobe was deployed on 22 September 2019, at an oblique angle facing a rock with a prominent sponge attached to it (Fig. 1; Supplement A; Table 1). The sponge was selected for its location approximately 31 m southeast of the well location, within the smallest radius of smothering observed in previous studies of drilling impact (Gates et al., 2019). The Nikon E995 camera was set to F 6.0, ISO 200, exposure 1/60, with photos of 2048 × 1536 pixels captured hourly. Images that were entirely obscured by suspended sediment were omitted from analysis (see below). The Seaguard single-point Recording Current Meter deep-water current meter was deployed on 23 September 2019 at approximately 5 m behind the time-lapse camera at approximately 0.7 m above seafloor, with sensors for current speed, direction and acoustic backscatter (1.9–2.0 MHz) in the water column. Data captured on the hour was used for analysis. Rolling means of the north and east components of the current speed across both 6- and 24-hour periods, centred on the middle time point, was calculated to represent both speed and direction. Similarly computed rolling means of the acoustic backscatter were used as a proxy for enhanced turbidity caused by suspended sediments at a depth of 0.7 m above seabed (at a distance of ~1.5–3.25 m). Seabed video of other sponge specimens at the site was captured in conjunction with the recovery of the time-lapse camera post-drilling, on 1 December 2019; lasers in the seabed video were spaced at 34 cm. Noteworthy moments in the time series are described semi-quantitatively. Correlations between data types are performed using all points in the time series.

2.2. Assessment of the sedimentation event

Qualitative information regarding the drilling activities was obtained from operational records, including the types of discharges. Quantification of sedimentation at the seabed as a result of drilling activities involved measurement of particles in the water column from backscatter and in the time-lapse images. Brightness (as mean RGB) was calculated for top left and top right corners (256 × 256 pixels; Supplement A) of each photo as a proxy of sediment in the water column. Photos where fish were visible in one or both top corners were removed from analysis. Brightness (as RGB values) in the selected areas was computed in R using the EBImage package (Pau et al., 2010). Mean RGB values were computed for each image. Rolling means for both backscatter and brightness across both 6- and 24-hour periods calculated centred on the middle time point.

2.3. Quantification of sediment accumulation on the sponge

Sediment accumulation on the sponge specimen was quantified using brightness detection of the sponge specimen in time-lapse images,

Table 1
Time-lapse photography details.

Deployment date and time	22 Sept 2019 12:04
Recovery date and time	9 Nov 2019 00:45
Image interval	1 h
Camera angle from seabed (theta)	25
Lens height above seabed	80 cm
Horizontal acceptance angle (in water; beta)	46
Vertical acceptance angle (alpha)	34
Field of view (see Supplement A)	0.9652 m^2
Total number of images	1141
Images with water column brightness detected	994
Images with sponge brightness detected	1072
Images with sponge apex location noted	1104

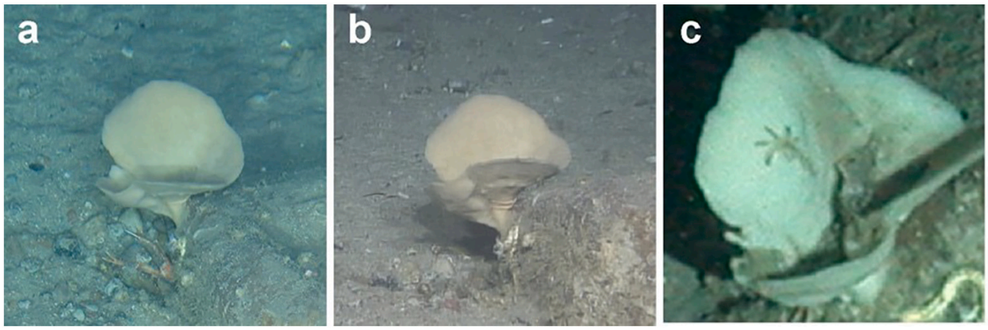

Fig. 1. The focal specimen of the study, a lamellate demosponge likely of the genus *Phakellia* or *Axinella*, (a,b) as observed from the side in a video captured with a remotely-operated vehicle pre-sedimentation event, and (c) in a time-lapse image with crustacean specimen evident on upper face of sponge.

where low brightness was used as a proxy for the accumulation of dark sediment on the light-coloured sponge. A portion of the sponge that was a large well-lit area facing the camera, not obscured by shadow nor affected by the movement of the sponge, was selected for brightness detection (Supplement A). This rectangular area was approximately 3600 pixels^2 (corner pixel coordinates: 1006.4, 724.8; 1028.9, 762.8; 1094.5, 715.5; 1072, 682.8), and was cropped from all images using Photoshop CS5. Brightness was computed as described for the top corners of the images (see above). Spearman's rank correlations were computed to assess relationships between the sponge brightness and the water column brightness and backscatter.

2.4. Quantification of sponge movement

To quantify movement of the sponge, the most prominent point to the top of the specimen was located in successive time-lapse images using the Video Annotation and Referencing System (Schlining and Stout, 2006). The distances between successive locations were computed in two-dimensional space, a simplification of the likely three-dimensional movement of the sponge. The resulting distances were assessed in pixel dimensions; real-world dimensions were difficult to determine because of the specimen's position an unknown distance above the seabed, with the camera in an oblique position.

3. Results

3.1. Sedimentation event

Records from Hurricane Energy indicated that drilling began on 24 September 2019, and that discharges from the drill rig were intermittent between 24 and 30 September 2019 (2 and 8 days after camera deployment). Contaminants discharged from the rig included barite drilling mud (M-I WATE; 834 tonnes), along with ethylene glycol, biocide, inhibitors, dispersants, cement and other additives (totalling 1064 tonnes discharged; Petrofac Facilities Management Limited, 2019a; Petrofac Facilities Management Limited, 2019b), along with 3332 tonnes of brine. The visible sedimentation material was likely a combination of drill mud (median particle size 6–75 μm) (MI Swaco, 2006), drill cuttings (971 t; Petrofac Facilities Management Limited, 2019a; Petrofac Facilities Management Limited, 2019b) and resuspended surface sediment.

At the seabed, water column brightness was initially 0.057 and backscatter was −41.2 dB prior to the start of the sedimentation event. These represent baseline and minimum values. Turbidity increased and deposition began to be observed at 25 Sept 2019, 2.5 days after the start of the camera deployment (Figs. 2 and 3). Three major peaks in sedimentation occurred at the beginning of the deployment (indicated by B–D in Fig. 2). The first and largest peak occurred at C, 6 days since deployment, with 24-h means of backscatter and water column brightness of −28.4 dB and 0.258 (4.5 times the initial brightness). The period of highest sedimentation occurred between B and E (4.9 to 7.7 days since deployment), during which the maximum 24-hourly mean backscatter and brightness reached −27.55 dB and 0.277. The greatest hourly backscatter and brightness reached were −0.28 dB (6.7 days since start) and 0.717 (2.6 days since start). The second peak in sedimentation (at F) was larger in the magnitude of 24-h mean backscatter (−30.95 dB; 9 % above the previous minimum at E) than in brightness (0.120; 3 % greater than at E and 47 % of the maximum at C). Following a period of reduced sedimentation, a third, sharp peak in sedimentation occurred again at point G, which was again greater in magnitude in 24-h mean backscatter (−30.73 dB, 90 % of the peak at F) than of brightness (0.083; 69 % of the peak at F and 32 % of the top peak at C). An extended period of minimal sediment in the water column was observed, with image brightness returning to approximately initial values by 14.8 days into the deployment, just prior to the peak around G, which lasted 48 h. This indication of low sedimentation was not observed in the backscatter data, which fluctuated erratically, punctuated by a smaller peak at J (−35.40 dB). The backscatter returned to the pre-J value around K and continued to fall until the end of the deployment. During the main sedimentation event (i.e., image brightness >0.06), backscatter and water column brightness were correlated ($\rho[298] = 0.66$, $p < 0.001$).

3.2. Sedimentation on the sponge

The specimen observed was a lamellate demosponge, likely of the genus *Phakellia* or *Axinella* (Fig. 1). The size of the specimen is more consistent with *Axinella*, but without examination of the spicules (silica skeletal elements), formal identification is impossible. A small crustacean was observed apparently living on the sponge. Across the period of observation, sponge colour (6-hour means) was correlated with backscatter ($\rho[1086] = -0.58$, $p < 0.0001$) and water column brightness ($\rho[1086] = -0.76$, $p < 0.0001$).

The sponge was not initially entirely sediment-free (brightness 0.283), potentially as a result of some sediment being deposited on it during rig arrival on site or camera deployment. Sediment accumulation on the sponge increased during drilling activity (2 days after camera deployment; between points A and B in Fig. 2b), resulting in a 6 % reduction in sponge brightness by point B. Sediment accumulation then increased dramatically when sediment in the water column was elevated (from B to C; visible in Fig. 3). At the peak of deposited sediment at point C (6 days after deployment start), sponge brightness was reduced by 24 % from its initial value. The sponge then brightened, suggesting that some accumulated sediment was removed, to a relative minimum at point E (7.7 days after deployment start), 22 % brighter than at the peak at C. Additional sediment accumulation on the sponge occurred, with a secondary peak at F (9.75 days). Accumulated sediment on the sponge then decreased, with a sharp decrease at G (15.9 days; 21 % brighter than at F). The sediment on the sponge continued to decrease, with the sponge becoming brighter than its initial condition at 17.8 days from deployment. Sediment on the sponge decreased faster between H and K

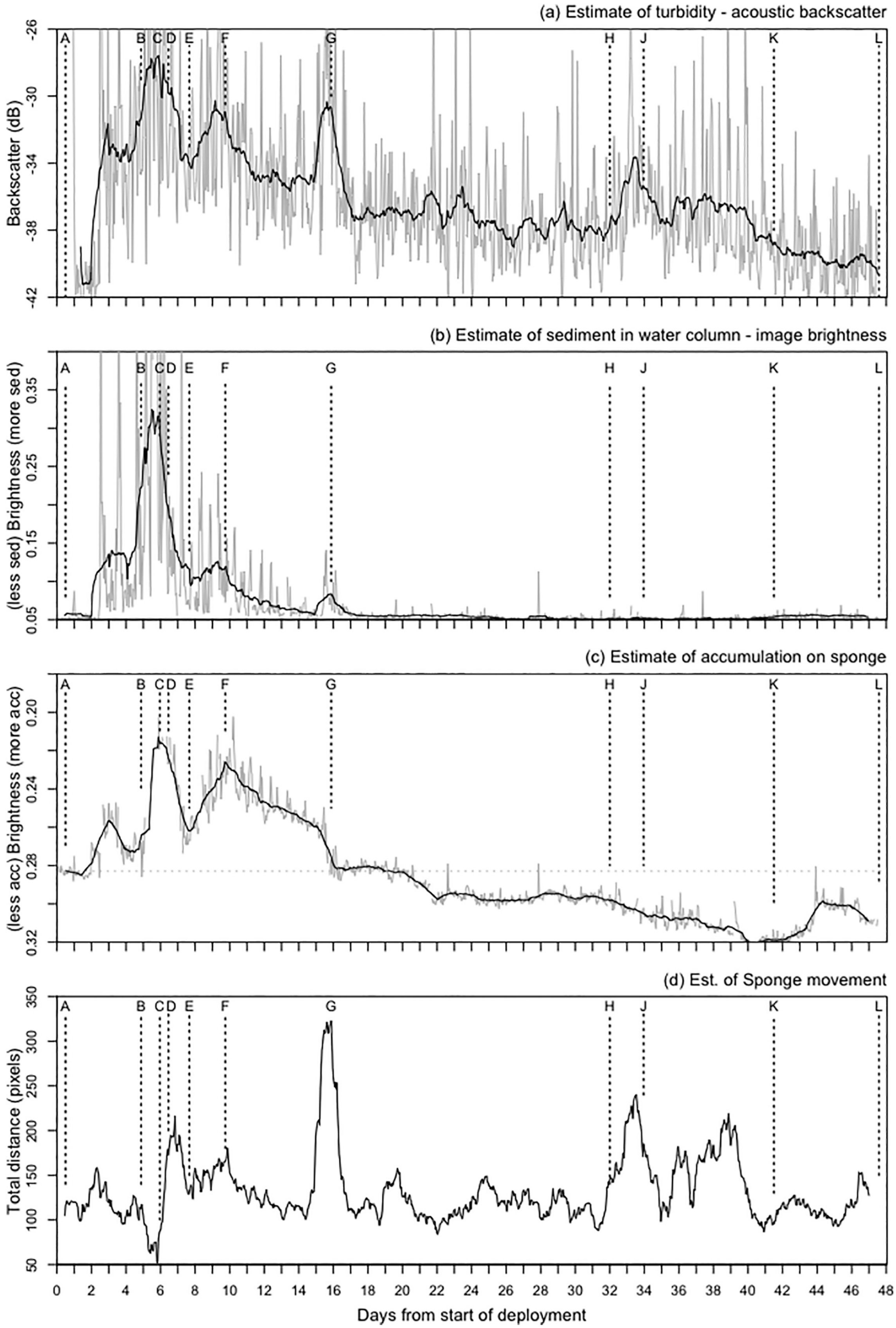

Fig. 2. Hourly (grey) and 24-hours rolling mean values (black) of (a) estimate of turbidity as acoustic backscatter, (b) estimates of sediment in the water column as brightness in image top corners. and (c) estimates of sedimentation on the sponge as reduction of brightness (with original brightness shows as horizontal dashed grey line). Estimated total movement of the sponge over 24-hours (d). Time points of interest (see Fig. 3) are indicated with vertical dashed lines, and labelled A-L. Y-axes are scaled to be representing the 24-h mean values, and some hourly values greatly exceed the y-axis maximum.

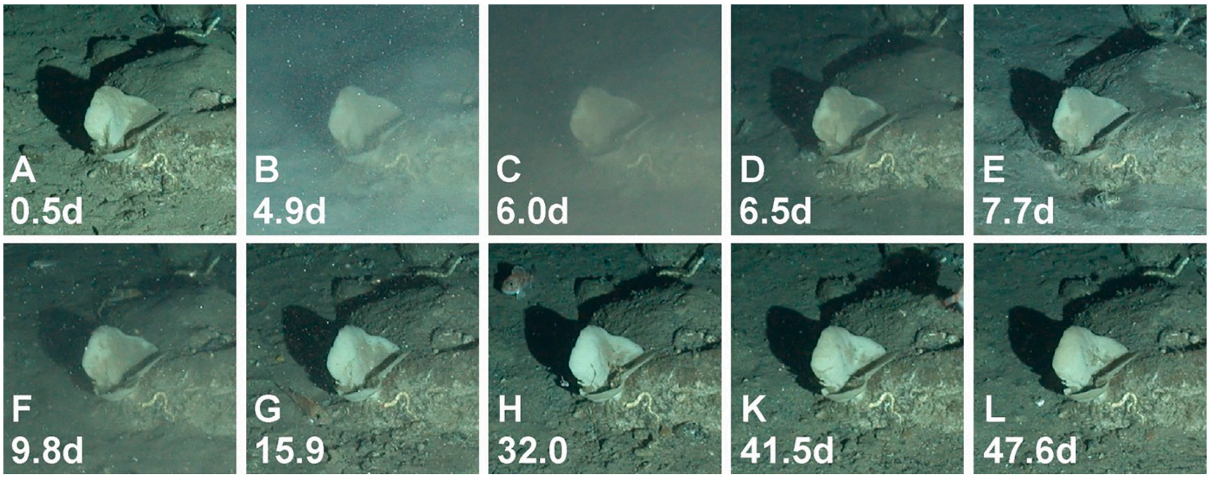

Fig. 3. Composite of images showing key moments in the time-lapse sequence of sedimentation and sponge recovery (letters denoting time points of interest from Fig. 2).

than immediately prior to or after this time.

Similar accumulations of sediment and drill cuttings were observed on other sponge specimens at distances of up to 100 m from the well centre (Fig. 4).

3.3. Sedimentation and sponge movement

The magnitude of sponge movement varied considerably across the deployment, and some movement events coincided with notable moments in the sedimentation event and in increase or decreases to the sediment visible on the sponge (Fig. 2). Initial sponge movement (at A) was 116 pixels (24-h mean). A reduction in sponge movement was observed near the first peak of sedimentation and accumulation on the sponge, between B and C; however, the position of the sponge was not visible in several photos in this period, so the observed drop may be erroneous. This was followed by a small peak in movement between C and E (24-h mean > 175 pixels), during the period of high accumulation on the sponge. Sponge movement increased again to a small peak at F (165 pixels), where another peak in sedimentation and accumulation occurred. Sponge movement then decreased steadily until a sharp peak at G (323 pixels; detailed observations in Fig. 5a), which coincided with a peak in sediment in the water column, and with a substantial brightening of the sponge. Following this peak, sponge movement returned to relatively low values. Sponge movement increased during the period between H and K (Fig. 5b), with a peak at J (214 pixels), corresponding to an increase in the backscatter. Sponge movement (6 h displacement) and sponge brightness were not correlated ($\rho[1086] = -0.026$, $p > 0.05$).

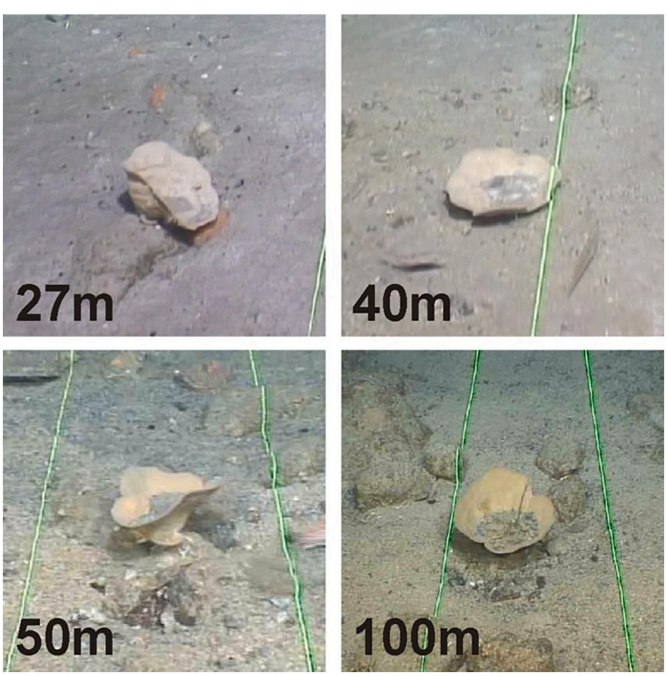

Fig. 4. Collected sediment and drill cuttings impacting sponge specimens of similar morphology, as observed in images extracted from seabed video at the site captured with a remotely-operated vehicle post-drilling activities. The distance of each specimen to the well centre is listed. Lasers were spaced at 34 cm.

3.4. Sponge movement and currents

The sponge moved continuously, with movement having an apparent tidal component (Fig. 6). Current speeds in the north and east directions (6-hour means) ranged from −8.9 to 10.9 cm s^{-1} and -17.5 to 20.3 cm s^{-1}, respectively, in the period A to G. Changes to variations in current speed coincided with notable sponge movement events. The peak in sponge movement around G occurred at the juncture between two-weekly tidal cycles, and when oscillations in the current speed were reduced and current speeds remained positive in both north and east components: the speed of north component of the current remained high immediately before G (3–9 cm s^{-1}), while the speed of the east component remained low (2–7 cm s^{-1}). The fluctuating increase in sponge movement between H and K occurred after the next juncture between neap/spring tidal cycles and coincided with the period greatest fluctuations in current speed: the greatest range in 6-h mean northerly (−12.2 to 14.1 cm s^{-1}) and easterly (−17.1 to 26.3 cm s^{-1}) components of current occurred then. At K, both the north and east components of the current were high, followed by a dip after J. Sponge movement (6 hourly displacement) was correlated with backscatter (6-h mean; $\rho[1086] = 0.26$, $p < 0.0001$).

4. Discussion

4.1. Characterisation of the sedimentation event

We relate the major peaks in sedimentation, observed as increases in the rolling mean backscatter and brightness over days (typically by 5–10 dB and 0.05 brightness, respectively), to discharges from the drilling activity. The fine-grained drill mud was likely to remain

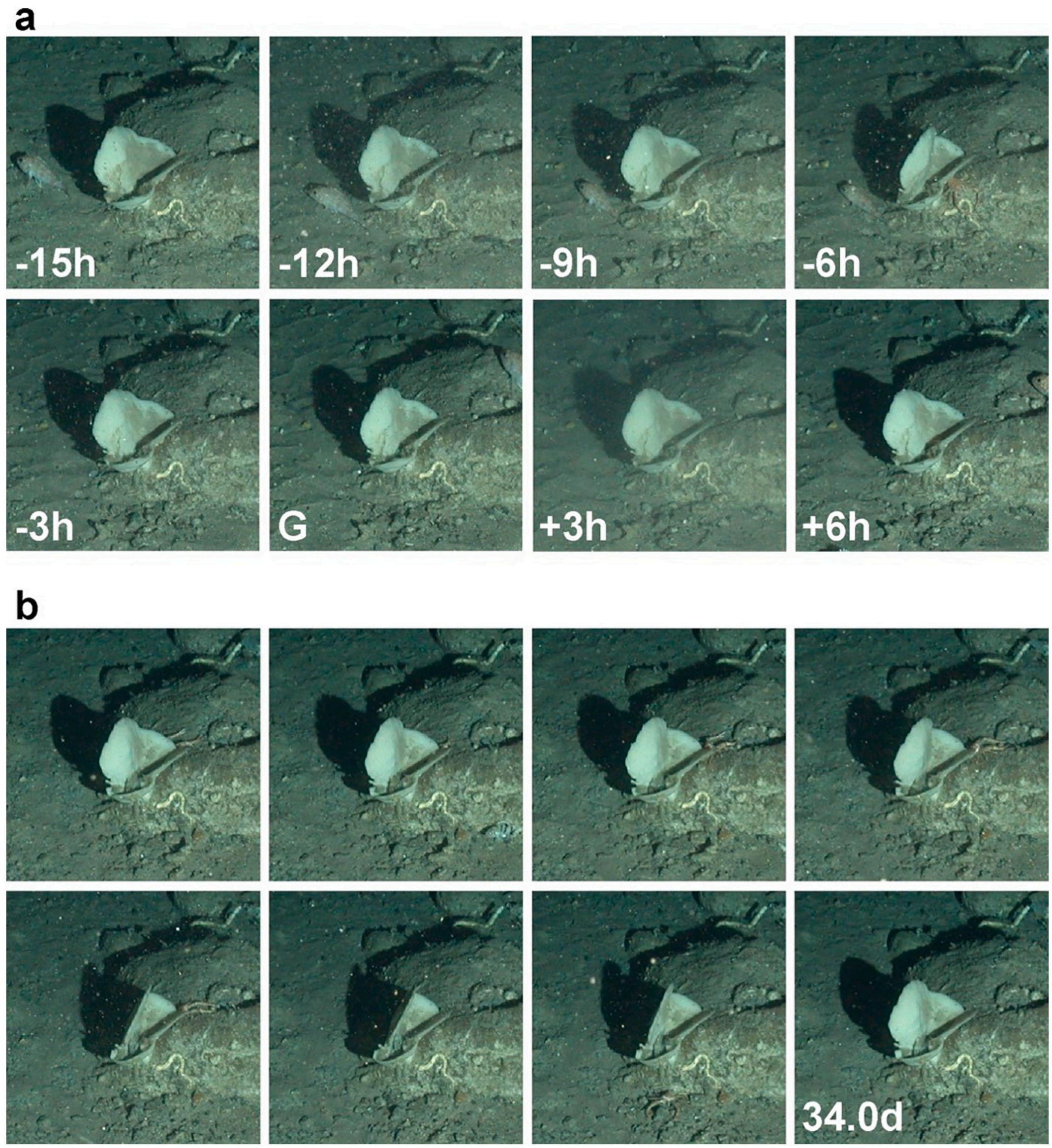

Fig. 5. Series of images of frequent and large sponge movement: (a) around peak of sedimentation and sustained northeast current speed at G, where sponge brightens substantially; (b) 3-hourly sequence during period of high backscatter and high variation in currents between points H–K (see Figs. 2 and 6).

suspended for extended periods, as the settling velocity of these grain sizes is slow (e.g. <0.005 ms^{-1}) (Hannah et al., 2006; Tedford et al., 2002). By contrast, the short-term spikes, with increases in backscatter >20 dB and brightness >0.3 over periods of ~1–4 h, were likely related to enhanced resuspension of coarser-grained sediments, the settling velocity of which would be much greater (e.g., ~0.07 ms^{-1} for particles 500 μm in size). These instances of shorter-lived sediment resuspension may be a result of the industrial activities and/or the tidally-modulated current movement that resuspended previously-deposited seafloor sediment.

The duration of the peaks in sedimentation and the materials involved have important implications for the effects on the sponge. Sponges are adapted to their local environments and natural background resuspension of local sediments, but may be impacted differently by drill mud as it is much finer than the coarse natural sediments. The relatively low settling speed of the drill mud results in an increased exposure time, in comparison to the resuspension of natural sediments. In addition, the particle size, shape and chemistry of the drill mud and cuttings likely also differ substantially from the natural sediment, and may include contaminants, with implications for clogging and physiological processes in the short and longer-term.

4.2. Recovery of the sponge from sedimentation

The sponge observed in this study was exposed to sedimentation over a period of ~6 days and was interpreted to have recovered visibly to its pre-drilling condition based on its colour 17.8 days after the start of sedimentation, with further recovery for another 14 days. In experimental settings, sponges have been observed to recover from acute or short-term exposures of hours to a few days (Pineda et al., 2017; Strehlow et al., 2017; Tjensvoll et al., 2013), while chronic or long-term exposures require longer recovery times, with some still not recovered 14 days post-exposure (Cummings et al., 2020; Mobilia et al., 2021; Strehlow et al., 2017). Long-term laboratory studies may also have protracted exposure periods or multiple exposures, but with recovery times of few days to 2 weeks. These comparisons highlight the exceptional length of exposure and of observed recovery time to acute impacts in our study. It is notable that the backscatter did not attenuate to pre-drilling values by the end of the observations in our study, suggesting that some drill mud remained suspended, resulting in longer-term

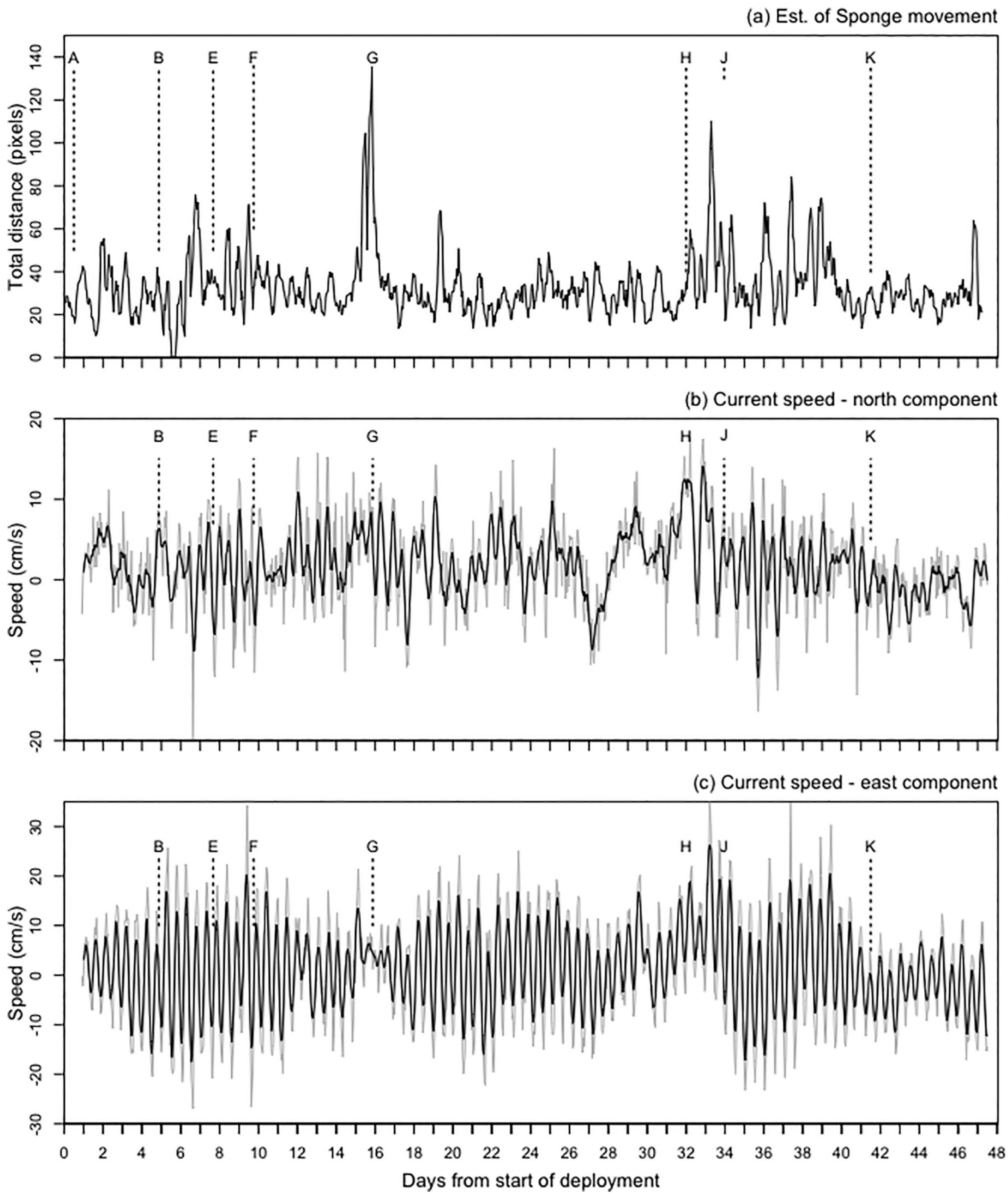

Fig. 6. Sum of sponge movement (a) over 6-hours, and current speeds as hourly (grey) and 6-hour rolling mean (black) of measured (b) north and (c) east components.

exposure.

Our observations indicate that drilling activity likely combines acute sedimentation impact during the initial period, from which at least partial recovery was observed, with chronic exposure evident from continued elevated backscatter. Direct comparisons between the recovery in these in-situ conditions to previous (laboratory) experiments is challenging because of the breadth of variables involved. Most previous studies involved shallow-water species of varying morphologies, used different types of sediment of varying particle sizes and concentrations, with exposure over short and longer time periods, and tested for recovery using a variety of metrics (e.g., visual, physiological). Here we focus on studies of visible impacts in morphologically-similar sponges, as recovery is morphology- and/or species-specific (Bell et al., 2015; Pineda et al., 2015; Pineda et al., 2017), to sedimentation by particles within the size range of the drilling mud. Pineda et al. (2015) found that massive and cup-shaped sponges were prone to impacts from sedimentation, with other erect morphologies less likely to be affected and faster to remove settled sediment. The same authors found that a wide cup-shaped sponge (*Carteriospongia foliascens*, with a similar morphology to *Phakellia*) that they studied was 80 % covered with fine sediment (63 μm in size) and recovered to 50 % coverage after 15 days. In another study, a thin, fan-shaped sponge (*Ianthella basta*) recovered from acute sediment exposure (18 μm for 48 h) within 3 days, while recovery from chronic exposure (29 μm for 4 weeks) took >2 weeks (Strehlow et al., 2017). The recovery times from these controlled experiments indicate that for combined acute and chronic types of sedimentation, such as was observed in our study, recovery may exceed 15 days, in line with our observations. Recovery may occur in stages, with some recovery from acute effects occurring at shorter timescales, followed by more prolonged recovery from chronic exposure, potentially as exposure continues. Observations of other sponge specimens at the site exposed to the sedimentation event provide evidence of longer-term impacts, with sediment and drill cuttings visible in the base of the 'cups' of specimens (Fig. 4). Our quantified observations focus on the erect portion of the sponge visible in the images, so such impacts are not considered. Future in-situ experiments should consider examining combined acute and chronic exposure.

Understanding the impacts of sedimentation on sponges is also dependent on knowledge of the concentration of suspended sediments to which a specimen is exposed. In real-world sedimentation events, such as the one observed in this study, sediment is dispersed from the source in space and time through settling and water movements. Laboratory studies often target particular concentrations (and/or particle sizes) of sediment with the aim of establishing thresholds for harm. A key paper in this regard is the sensitivity study identified a sediment burial threshold of 6.3 mm for benthic species through a literature review (Smit et al., 2008). This threshold has subsequently been referenced in experimental studies on suspension-feeders (Allers et al., 2013; Larsson and Purser, 2011). However, the burial depth threshold of 6.3 mm does not align to field observations near oil and gas drilling sites (Norwegian Pollution Control Authority, 2008; Trannum et al., 2010). Furthermore, using a burial threshold has two major limitations: (1) it does not directly relate to the concentration of sediment and drill muds particles in suspension in the water, (2) it does not allow for simple quantification in the field, such as in seabed images or videos. Therefore, there is a need to move away from the burial threshold measurement towards metrics that can be measured through imagery surveys and reflect exposure severity, such as estimates of sediment concentrations in suspension. Direct comparison of the observations in this study with those of laboratory-based studies is precluded by a lack of direct calibration of backscatter and brightness to define absolute sediment concentrations, but some insight into the chronic exposure may be gained from other studies that deployed a similar acoustic instrument. In such a study, where full backscatter attenuation also did not occur, suspended sediment concentrations of ~1–3 mg L^{-1} were recorded (e.g., Zhang et al., 2014). Similar concentrations may thus be applicable at our site; however, this value will likely vary based on differences in particle size (e.g., Haalboom et al., 2021; Thorne and Hanes, 2002). This concentration range is lower than the concentrations used in many experimental studies. For example, physiological responses, including reductions in respiration and filtration, have been observed at concentrations of 10–80 mgL^{-1} (Grant et al., 2018; Kutti et al., 2015; Mobilia et al., 2021; Tjensvoll et al., 2013). This points to the importance of studying the impacts of longer-term exposures at lower concentrations, as observed in the latter portion of this study, as these exposures were found to have more permanent effects (Kutti et al., 2015). In addition, establishing calibrations between measured sediment concentrations and in-situ measurements (e.g., backscatter or brightness) will be important to better quantifying the impacts of sedimentation using in-situ sensors. Regardless, our study provides a valuable link between observed sediment suspensions and the effects on a sponge in a real-world setting.

4.3. Backscatter and image brightness as representations of sedimentation impact

In the absence of any physical calibration, we cannot provide a robust conversion of acoustic backscatter to absolute suspended sediment concentration, and such an inversion is sensitive to both temporal and vertical changes in grain size and density (Moate and Thorne, 2012; Thorne and Hanes, 2002; Thorne et al., 2011). However, the observed changes in acoustic backscatter based on prior studies that have considered similar frequency instruments provide some context. The Seaguard RCM operates in the 1.9–2.0 MHz band, which is equivalent to a wavelength of 750 μm. At this wavelength, Doppler current profilers have a maximum sensitivity for particles of diameter 238 μm, and can detect particles down to diameter 60 μm, for which backscatter power is <1/10 of peak backscatter power (Guerrero et al., 2012; Guerrero et al., 2011; Henry et al., 2021). The Seaguard RCM should therefore be mostly sensitive to the presence of sand-sized particles, larger than 60 μm. As the drilling mud was fine-grained (median particle size 6–75 μm), much of this material may fall below the theoretically detectable limits of the Doppler Current Sensor. By contrast, the natural sediment at the site is extremely variable spatially, but generally much coarser than the drill mud. Thus, it is likely that these coarser natural sediments will provide a more distinct signature in the recorded backscatter data, while the frequency used may not adequately record the finer drill mud. Detection of sediments in the backscatter data may also be biased by the sediment moving towards the sensor in particular directions of current flow, or when sediment is more prone to resuspension by higher bed shear stresses. Future experiments should consider an array of current meters, including multiple frequencies of instrument appropriate to the anticipated particle size range along with sediment traps or settling plates to provide calibration to quantitatively link acoustic backscatter and brightness in photographs to sediment concentrations.

The backscatter and image brightness measures of turbidity did not match across the period of observation. Correlation between the two metrics during the main sedimentation period suggests that brightness detection in seabed photography may be a reasonable method for detecting heavy sedimentation. However, this method missed the elevated backscatter during the later period of observation. In addition, sponge colour was correlated to backscatter and not brightness. These results suggest that the backscatter likely detected particles that were not visible in the image brightness, in this case the natural sediment may not be detected well in the image brightness. Thus, it is likely that the particles detected only in the backscatter originated as drill mud rather than from the local sediment.

The impact of these small particles, potentially from the drill mud, was likely also missed from our assessment of sponge impact using photographic methods. Firstly, image-based methods only detect visible changes to the exterior of the specimen, so internal impacts, which are known results of sedimentation on sponges (Cummings et al., 2020), are neglected. In addition, larger particles collecting on the surface of the sponge provide more substantial colour change and would be more readily detected using the brightness method. Observed changes to sponge colour likely reflect either the collection of large particles or heavy deposition of small particles, so both the sedimentation and the recovery estimates using this method likely underestimate the true changes. Thus, the image brightness approach may detect acute heavy sedimentation rather than lower concentration chronic impacts. While seabed imaging is gaining popularity as a cost-effective method for monitoring the health seabed habitats, providing the ability to assess water column sedimentation, deposition and movement behaviour, these limitations in detecting smothering impacts should be considered.

4.4. Possible mechanisms of sponge recovery

The recovery of the sponge involved brightening, which is interpreted to be a result of removal of sediment from the surface of the sponge. This mostly occurred gradually, but with notable inflection points where appreciable brightening occurred rapidly. For example, the rapid removal of sediment within a few hours at point G, coinciding with an increase in sediment in the water column. The mechanisms employed by *Axinella* or *Phakellia* sponges for the removal of sediment are unknown, but other species use mucous production, exclusion of particles by incurrent pores, closing of oscula and ceasing pumping, expulsion of particles from aquiferous system, reducing their aquiferous system volume, and tissue sloughing (Barthel and Wolfrath, 1989; Strehlow et al., 2017). Mechanisms by which sponges remove local sediments may (or may not) be suitable for removing drill mud, with its different composition, particle size and shape, and concentrations.

Active behaviours to remove sediment have also been observed, including “coughing” and “sneezing” of mucous, with contractions in ~20–50 min (Grant et al., 2018; Kornder et al., 2022). These types of behaviour may be the reason for the sudden change in sponge colour, despite the lack of correlation between sponge movement and brightness, because the hourly image interval was too long to capture such behaviour. Active behaviours involving movement may be reduced in specimens with substantial ballasting from depositing drill cuttings or rock chips, such as those observed near the site (Fig. 4).

The mechanism for sediment removal may have been passive, as a result of changes in current speed and direction. Alterations to the current speed and direction at point G and in the period between H and K, particularly at short intervals, may have induced sediment removal and sponge brightening. The correlation of the movement of the sponge to the backscatter, may be related to the changes current speed and direction resulting in resuspension of fine material. Sponge movement in this case may be passive as the result of currents, or active in response to them. However, the frequency of images does not facilitate investigation of the relative roles of active and passive sediment removal mechanisms in detail. Sediment removal may also have been enabled by the crustacean observed living on the sponge, as this mechanism has been observed for other mutualist relationships with sponges (Hendler, 1984; Henkel and Pawlik, 2014). Mutualist and active sediment removal may be important recovery for sponges in habitats in less vigorous hydrodynamic settings, where passive removal by currents may be limited, such as the abyssal seafloor targeted for mining (e.g., Durden et al., 2021; Herzog et al., 2018; Kersken et al., 2017; Simon-Lledó et al., 2019).

5. Conclusion

This study contributes an important in-situ observation of the response of a sponge to a real-world hydrocarbon drilling event. It adds to a growing body of evidence of the impacts of industrial sedimentation to sponges. In-situ observing is necessary for understanding the impacts to deep-sea species that cannot be brought to the surface for laboratory experiments. Similarly, in-situ observing is critical to monitoring industrial impacts to those organisms in remote habitats, particularly as sediment-generating industrial activities increasingly target deep water over vast areas (Aleynik et al., 2017) and local hydrodynamic conditions could extend fine-grained sediment plumes to distances of hundreds of kilometres (Bradshaw et al., 2012; Durrieu De Madron et al., 2005; Schoellhamer, 1996). The combination of laboratory studies and in-situ observations provide valuable quantifications of the impacts, responses and potential for recovery for benthic organisms that will be important for the designation of conservation actions and to conducting environmental risk and impact assessments for hydrocarbon drilling, dredging, trawling and deep-sea mining. Collaborations with these industries to monitor the impacts of trial work should be encouraged. Finally, in-situ observations of impact and recovery from sedimentation will be important in understanding the intersection of sedimentation with other industrial and climate change impacts, as the pressures on sponges and marine organisms accumulate (Levin et al., 2020; Washburn et al., 2019).

Supplementary data to this article can be found online at https://doi.org/10.1016/j.marpolbul.2023.114870.

CRediT authorship contribution statement

Durden: Conceptualization, Methodology, Investigation, Formal Analysis, Data Curation, Writing – Original Draft **Clare:** Formal Analysis, Writing-Reviewing and Editing **Vad:** Writing-Reviewing and Editing **Gates:** Conceptualization, Methodology, Writing-Reviewing and Editing, Funding acquisition.

Declaration of competing interest

The authors declare the following financial interests/personal relationships which may be considered as potential competing interests: Jennifer Durden, Andrew Gates report financial support provided by Hurricane Energy. Jennifer Durden, Andrew Gates, Michael Clare report financial support provided by UK NERC. Jennifer Durden, Johanne Vad report financial support was provided by EU Horizon 2020.

Data availability

Data from this study are available in PANGAEA (doi: https://doi.org/10.1594/PANGAEA.955147): Durden and Gates (2022).

Acknowledgements

We thank Hurricane Energy, the Oceaneering remotely-operated vehicle team and the platform crew of the Transocean Leader for supporting field operations. This work was supported by Hurricane Energy as part of the SERPENT project, the UK Natural Environment Research Council Climate Linked Atlantic Sector Science project (NE/R015953/1), and by the European Union's Horizon 2020 research and innovation programme iAtlantic project (No. 818123). This paper reflects the authors' view alone and the European Union cannot be held responsible for any use that may be made of the information contained herein.

References

Aleynik, D., Inall, M.E., Dale, A.C., Vink, A., 2017. Impact of remotely generated eddies on plume dispersion at abyssal mining sites in the Pacific. Sci. Rep. 7, 16959. https://doi.org/10.1038/s41598-017-16912-2.

Allers, E., Abed, R.M.M., Wehrmann, L.M., Wang, T., Larsson, A.I., Purser, A., de Beer, D., 2013. Resistance of Lophelia Pertusa to coverage by sediment and petroleum drill cuttings. Mar. Pollut. Bull. 74, 132–140. https://doi.org/10.1016/J.MARPOLBUL.2013.07.016.

Bannister, R.J., Battershill, C.N., de Nys, R., 2012. Suspended sediment grain size and mineralogy across the continental shelf of the great barrier reef: impacts on the physiology of a coral reef sponge. Cont. Shelf Res. 32, 86–95. https://doi.org/10.1016/j.csr.2011.10.018.

Barthel, D., Wolfrath, B., 1989. Tissue sloughing in the sponge Halichondria panicea: a fouling organism prevents being fouled. Oecologia 78, 357–360. https://doi.org/10.1007/BF00379109.

Beaulieu, S.E., 2001. Life on glass houses: sponge stalk communities in the deep sea. Mar. Biol. 138, 803–817. https://doi.org/10.1007/s002270000500.

Bell, J.J., McGrath, E., Biggerstaff, A., Bates, T., Bennett, H., Marlow, J., Shaffer, M., 2015. Sediment impacts on marine sponges. Mar. Pollut. Bull. 94, 5–13. https://doi.org/10.1016/j.marpolbul.2015.03.030.

Bett, B.J., 2001. UK Atlantic margin environmental survey: introduction and overview of bathyal benthic ecology. Cont. Shelf Res. 21, 917–956.

Bett, B.J., 2012. Seafloor Biotope Analysis of the Deep Waters of the SEA4 Region of Scotland's Seas. Vol. Report No. 472. Joint Nature Conservation Committee.

Bett, B.J., Rice, A.L., 1992. The influence of hexactinellid sponge (Pheronema-Carpenteri) spicules on the patchy distribution of macrobenthos in the porcupine seabight (Bathyal ne Atlantic). Ophelia 36, 217–226.

Bradshaw, C., Tjensvoll, I., Skold, M., Allan, I.J., Molvaer, J., Magnusson, J., Naes, K., Nilsson, H.C., 2012. Bottom trawling resuspends sediment and releases bioavailable contaminants in a polluted fjord. Environ. Pollut. 170, 232–241. https://doi.org/10.1016/j.envpol.2012.06.019.

Cathalot, C., Van Oevelen, D., Cox, T.J.S., Kutti, T., Lavaleye, M., Duineveld, G., Meysman, F.J.R., 2015. Cold-water coral reefs and adjacent sponge grounds: hotspots of benthic respiration and organic carbon cycling in the deep sea. Front. Mar. Sci. 2 https://doi.org/10.3389/fmars.2015.00037.

Cummings, V.J., Beaumont, J., Mobilia, V., Bell, J.J., Tracey, D., Clark, M.R., Barr, N., 2020. Responses of a common New Zealand coastal sponge to elevated suspended sediments: indications of resilience. Mar. Environ. Res. 155, 104886 https://doi.org/10.1016/j.marenvres.2020.104886.

Durden, J.M., Gates, A.R., 2022. Observations of sedimentation from hydrocarbon drilling and impacts to a sponge specimen. PANGAEA. https://doi.org/10.1594/PANGAEA.955147.

Durden, J.M., Lallier, L.E., Murphy, K., Jaeckel, A., Gjerde, K., Jones, D.O.B., 2018. Environmental impact assessment process for deep-sea mining in 'the area'. Mar. Policy 87, 194–202. https://doi.org/10.1016/j.marpol.2017.10.013.

Durden, J.M., Putts, M., Bingo, S., Leitner, A.B., Drazen, J.C., Gooday, A.J., Jones, D.O.B., Sweetman, A.K., Washburn, T.W., Smith, C.R., 2021. Megafaunal ecology of the

Western clarion clipperton zone. Front. Mar. Sci. 8 https://doi.org/10.3389/fmars.2021.671062.
Durrieu De Madron, X., Ferre, B., Le Corre, G., Grenz, C., Conan, P., Pujo Pay, M., Buscail, R., Bodiot, O., 2005. Trawling-induced resuspension and dispersal of muddy sediments and dissolved elements in the Gulf of lion (NW Mediterranean). Cont. Shelf Res. 25, 2387–2409. https://doi.org/10.1016/j.csr.2005.08.002.
Gates, A., Durden, J., 2021. SERPENT Activity Report: Lincoln 205/26b-14 and Warwick Crestal. 2019. UK. National Oceanography Centre Cruise Report, No. 75. National, Southampton, UK.
Gates, A.R., Horton, T., Serpell-Stevens, A., Chandler, C., Grange, L.J., Robert, K., Bevan, A., Jones, D.O.B., 2019. Ecological role of an offshore industry artificial structure. Front. Mar. Sci. 6 https://doi.org/10.3389/fmars.2019.00675.
Gates, A.R., Jones, D.O., 2012. Recovery of benthic megafauna from anthropogenic disturbance at a hydrocarbon drilling well (380 m depth in the Norwegian Sea). Plos One 7, e44114. https://doi.org/10.1371/journal.pone.0044114.
GEOXYZ Benthic Solutions, 2019a. In: Warwick Crestal Habitat Assessment. GEOXYZ Benthic Solutions, p. 64.
GeoXYZ Benthic Solutions, 2019b. In: Warwick Field Environmental Baseline Survey Results. GEOXYZ Benthic Solutions, p. 144.
Gollner, S., Kaiser, S., Menzel, L., Jones, D., Brown, A., Mestre, N., Oevelen, D.V., Menot, L., Colaço, A., Canals, M., Cuvelier, D., Durden, J., Gebruk, A., Aruoriwo, E., Haeckel, M., Marcon, Y., Mevenkamp, L., Morato, T., Pham, C., Purser, A., Sanchez-Vidal, A., Vanreusel, A., Vink, A., Arbizu, P.M., 2017. Resilience of benthic deep-sea fauna to mining activities. Mar. Environ. Res. 129, 76–101.
Grant, N., Matveev, E., Kahn, A.S., Leys, S.P., 2018. Suspended sediment causes feeding current arrests in situ in the glass sponge Aphrocallistes vastus. Mar. Environ. Res. 137, 111–120. https://doi.org/10.1016/j.marenvres.2018.02.020.
Guerrero, M., Rüther, N., Szupiany, R.N., 2012. Laboratory validation of acoustic doppler current profiler (ADCP) techniques for suspended sediment investigations. Flow Meas. Instrum. 23, 40–48.
Guerrero, M., Szupiany, R.N., Amsler, M., 2011. Comparison of acoustic backscattering techniques for suspended sediments investigation. Flow Meas. Instrum. 22, 392–401.
Haalboom, S., de Stigter, H., Duineveld, G., van Haren, H., Reichart, G.-J., Mienis, F., 2021. Suspended particulate matter in a submarine canyon (Whittard canyon, Bay of Biscay, NE Atlantic Ocean): assessment of commonly used instruments to record turbidity. Mar. Geol. 434 https://doi.org/10.1016/j.margeo.2021.106439.
Hannah, C.G., Drozdowski, A., Loder, J., Muschenheim, K., Milligan, T., 2006. An assessment model for the fate and environmental effects of offshore drilling mud discharges. Estuar. Coast. Shelf Sci. 70, 577–588.
Hendler, G., 1984. The association of Ophiothrix lineata and Callyspongia vaginalis; a brittlestar-sponge cleaning symbiosis? Mar. Ecol. 5, 9–27.
Henkel, T.P., Pawlik, J.R., 2014. Cleaning mutualist or parasite? Classifying the association between the brittlestar Ophiothrix lineata and the Caribbean reef sponge Callyspongia vaginalis. J. Exp. Mar. Biol. Ecol. 454, 42–48. https://doi.org/10.1016/J.JEMBE.2014.02.005.
Henry, P., Özeren, S., Yakupoğlu, N., Çakir, Z., de Saint-Léger, E., Desprez de Gésincourt, O., Tengberg, A., Chevalier, C., Papoutsellis, C., Postacıoğlu, N., Dogan, U., 2021. Slow build-up of turbidity currents triggered by a moderate earthquake in the Sea of Marmara. Nat. Hazards Earth Syst. Sci. Discuss. 1–28.
Herzog, S., Amon, D.J., Smith, C.R., Janussen, D., 2018. Two new species of sympagella (Porifera: hexactinellida: Rossellidae) collected from the clarion-clipperton zone, East Pacific. Zootaxa 4466, 152–163. https://doi.org/10.11646/zootaxa.4466.1.12.
Joint Nature Conservation Committee, 2014a. Faroe-Shetland Sponge Belt MPA: Site Summary Document. Joint Nature Conservation Committee.
Joint Nature Conservation Committee, 2014b. West Shetland Shelf MPA: Site Summary Document. Joint Nature Conservation Committee.
Jones, D.O.B., Gates, A.R., Lausen, B., 2012. Recovery of deep-water megafaunal assemblages from hydrocarbon drilling disturbance in the Faroe−Shetland Channel. Mar. Ecol. Prog. Ser. 461, 71–82. https://doi.org/10.3354/meps09827.
Jones, D.O.B., Hudson, I.R., Bett, B.J., 2006. Effects of physical disturbance on the cold-water megafaunal communities of the faroe-Shetland Channel. Mar. Ecol. Prog. Ser. 319, 43–54.
Jones, D.O.B., Kaiser, S., Sweetman, A.K., Smith, C.R., Menot, L., Vink, A., Trueblood, D., Greinert, J., Billett, D.S.M., Martinez Arbizu, P., Radziejewska, T., Singh, R., Ingole, B., Stratmann, T., Simon-Lledo, E., Durden, J.M., Clark, M.R., 2017. Biological responses to disturbance from simulated deep-sea polymetallic nodule mining. PLoS ONE 12, e0171750. https://doi.org/10.1371/journal.pone.0171750.
Kazanidis, G., Vad, J., Henry, L.-A., Neat, F., Berx, B., Georgoulas, K., Roberts, J.M., 2019. Distribution of Deep-Sea sponge aggregations in an area of multisectoral activities and changing oceanic conditions. Front. Mar. Sci. 6 https://doi.org/10.3389/fmars.2019.00163.
Kenchington, E., Power, D., Koen-Alonso, M., 2013. Associations of demersal fish with sponge grounds on the continental slopes of the Northwest Atlantic. Mar. Ecol. Prog. Ser. 477, 217–230. https://doi.org/10.3354/meps10127.
Kersken, D., Janussen, D., Martínez Arbizu, P., 2017. Deep-sea glass sponges (Hexactinellida) from polymetallic nodule fields in the clarion-clipperton fracture zone (CCFZ), northeastern Pacific: part I – amphidiscophora. Mar. Biodivers. https://doi.org/10.1007/s12526-017-0727-y.
Kornder, N.A., Esser, Y., Stoupin, D., Leys, S.P., Mueller, B., Vermeij, M.J.A., Huisman, J., de Goeij, J.M., 2022. Sponges sneeze mucus to shed particulate waste from their seawater inlet pores. Curr. Biol. https://doi.org/10.1016/j.cub.2022.07.017.
Kutti, T., Bannister, R.J., Fosså, J.H., Krogness, C.M., Tjensvoll, I., Søvik, G., 2015. Metabolic responses of the deep-water sponge Geodia barretti to suspended bottom sediment, simulated mine tailings and drill cuttings. J. Exp. Mar. Biol. Ecol. 473, 64–72. https://doi.org/10.1016/j.jembe.2015.07.017.
Laguionie-Marchais, C., Kuhnz, L.A., Huffard, C.L., Ruhl, H.A., Smith Jr., K.L., 2015. Spatial and temporal variation in sponge spicule patches at station M, Northeast Pacific. Mar. Biol. 162, 617–624. https://doi.org/10.1007/s00227-014-2609-1.
Larsson, A.I., Purser, A., 2011. Sedimentation on the cold-water coral Lophelia Pertusa: cleaning efficiency from natural sediments and drill cuttings. Mar. Pollut. Bull. 62, 1159–1168. https://doi.org/10.1016/J.MARPOLBUL.2011.03.041.
Levin, L.A., Wei, C.L., Dunn, D.C., Amon, D.J., Ashford, O.S., Cheung, W.W.L., Colaco, A., Dominguez-Carrio, C., Escobar, E.G., Harden-Davies, H.R., Drazen, J.C., Ismail, K., Jones, D.O.B., Johnson, D.E., Le, J.T., Lejzerowicz, F., Mitarai, S., Morato, T., Mulsow, S., Snelgrove, P.V.R., Sweetman, A.K., Yasuhara, M., 2020. Climate change considerations are fundamental to management of deep-sea resource extraction. Glob. Chang. Biol. 26, 4664–4678. https://doi.org/10.1111/gcb.15223.
Lohrer, A.M., Hewitt, J.E., Thrush, S.F., 2006. Assessing far-field effects of terrigenous sediment loading in the coastal marine environment. Mar. Ecol. Prog. Ser. 315, 13–18.
Maldonado, M., Aguilar, R., Bannister, R.J., Bell, J.J., Conway, K.W., Dayton, P.K., Díaz, C., Gutt, J., Kelly, M., Kenchington, E.L.R., Leys, S.P., Pomponi, S.A., Rapp, H. T., Rützler, K., Tendal, O.S., Vacelet, J., Young, C.M., 2015. Sponge grounds as key marine habitats: a synthetic review of types, structure, functional roles, and conservation concerns. Mar. Anim. For. 1–39.
Maldonado, M., Giraud, K., Carmona, C., 2008. Effects of sediment on the survival of asexually produced sponge recruits. Mar. Biol. 154, 631–641.
Maldonado, M., Ribes, M., van Duyl, F.C., 2012. Nutrient fluxes through sponges: biology, budgets, and ecological implications. Adv. Mar. Biol. 30 (62), 113–182. https://doi.org/10.1016/B978-0-12-394283-8.00003-5.
MI Swaco, 2006. M-I Wate High-quality Barite Product Sheet. slb.com.
Mitchell, E.G., Harris, S., 2020. Mortality, population and community dynamics of the glass sponge dominated community “the forest of the weird” from the Ridge Seamount, Johnston Atoll, Pacific Ocean. Front. Mar. Sci. 7, 565171 https://doi.org/10.3389/fmars.2020.565171.
Moate, B.D., Thorne, P.D., 2012. Interpreting acoustic backscatter from suspended sediments of different and mixed mineralogical composition. Cont. Shelf Res. 46, 67–82.
Mobilia, V., Cummings, V.J., Clark, M.R., Tracey, D., Bell, J.J., 2021. Short-term physiological responses of the New Zealand deep-sea sponge Ecionemia novaezealandiae to elevated concentrations of suspended sediments. J. Exp. Mar. Biol. Ecol. 541 https://doi.org/10.1016/j.jembe.2021.151579.
Norwegian Pollution Control Authority, 2008. Kostnader og nytte for miljø og samfunnved å stille krav om injeksjon/reinjeksjon av produsert vann, nullutslipp avborekaks og borevæske og inkludere radioaktivitet i nullutslippsmålet. Norwegian.SFT report TA-2468/2008.
OSPAR Commission, 2010. In: Background Document fo Deep-sea Sponge Aggregations. Biodiversity series. OSPAR Commission, London, p. 46.
Pau, G., Fuchs, F., Sklyar, O., Boutros, M., Huber, W., 2010. EBImage—an R package for image processing with applications to cellular phenotypes. Bioinformatics 26, 979–981. https://doi.org/10.1093/bioinformatics/btq046.
Petrofac Facilities Management Limited, 2019a. OPPC Well Permit: Well No. 204/30b-4 OPPC Permit OTP/893/2/1 Chemical Permit CP/2095/2/1. Environmental Emissions Monitoring System report: UK Government Department of Business, Energy, Industrial Strategy.
Petrofac Facilities Management Limited, 2019b. Use of Drilling Fluids and Cuttings Summary: Well No. 204/30b-4 Permit CP/2095/2/1. Environmental Emissions Monitoring System Report: UK Government Department of Business, Energy, Industrial Strategy.
Pineda, M.C., Duckworth, A., Webster, N., 2015. Appearance matters: sedimentation effects on different sponge morphologies. J. Mar. Biol. Assoc. U. K. 96, 481–492. https://doi.org/10.1017/s0025315414001787.
Pineda, M.C., Strehlow, B., Sternel, M., Duckworth, A., Haan, J.D., Jones, R., Webster, N. S., 2017. Effects of sediment smothering on the sponge holobiont with implications for dredging management. Sci. Rep. 7, 5156. https://doi.org/10.1038/s41598-017-05243-x.
Pusceddu, A., Bianchelli, S., Martín, J., Puig, P., Palanques, A., Masqué, P., Danovaro, R., 2014. Chronic and intensive bottom trawling impairs deep-sea biodiversity and ecosystem functioning. Proc. Natl. Acad. Sci. U. S. A. 111, 8861–8866. https://doi.org/10.1073/pnas.1405454111.
Roberts, D.E., Davis, A.R., Cummins, S.P., 2006. Experimental manipulation of shade, silt, nutrients and salinity on the temperate reef sponge Cymbastela concentrica. Mar. Ecol. Prog. Ser. 307, 143–154.
Roegner, G.C., Fields, S.A., Henkel, S.K., 2021. Benthic video landers reveal impacts of dredged sediment deposition events on mobile epifauna are acute but transitory. J. Exp. Mar. Biol. Ecol. 538 https://doi.org/10.1016/j.jembe.2021.151526.
Schlining, B.M., Stout, N.J., 2006. In: MBARI’s Video Annotation and Reference System. OCEANS 2006. IEEE, Boston, USA, pp. 1–5.
Schoellhamer, D.H., 1996. Anthropogenic sediment resuspension mechanisms in a shallow microtidal estuary. Estuar. Coast. Shelf Sci. 43, 533–548. https://doi.org/10.1006/ecss.1996.0086.
Simon-Lledó, E., Bett, B.J., Huvenne, V.A.I., Schoening, T., Benoist, N.M.A., Jeffreys, R. M., Durden, J.M., Jones, D.O.B., 2019. Megafaunal variation in the abyssal landscape of the clarion clipperton zone. Prog. Oceanogr. 170, 119–133. https://doi.org/10.1016/j.pocean.2018.11.003.
Smit, M.G.D., Holthaus, K.I.E., Trannum, H.C., Neff, J.M., Kjeilen-Eilertsen, G., Jak, R.G., Singsaas, I., Huijbregts, M.A.J., Hendriks, A.J., 2008. Species sensitivity distributions for suspended clays, sediment burial, and grain size change in the marine environment. Environ. Toxicol. Chem. 27, 1006–1012. https://doi.org/10.1897/07-339.1.

Strehlow, B.W., Pineda, M.C., Duckworth, A., Kendrick, G.A., Renton, M., Abdul Wahab, M.A., Webster, N.S., Clode, P.L., 2017. Sediment tolerance mechanisms identified in sponges using advanced imaging techniques. PeerJ 5, e3904. https://doi.org/10.7717/peerj.3904.

Taboada, S., Whiting, C., Wang, S., Ríos, P., Davies, A., Mienis, F., Kenchington, E., Cárdenas, P., Cranston, A., Koutsouveli, V., Cristobo, J., Rapp, H.-T., Drewery, J., Baldó, F., Morrow, C., Picton, B., Xavier, J., Arias, M.B., Riesgo, A., 2022. Connectivity of sponge grounds in the deep sea: genetic diversity, gene flow and oceanographic pathways in the fan-shaped sponge Phakellia ventilabrum in the Northeast Atlantic. Authorea. https://doi.org/10.22541/au.164873620.02723929/v1.

Tedford, T., Hannah, C.G., Milligan, T.G., Loder, J.W., Muschenheim, D.K., 2002. Flocculation and the fate of drill mud discharges. Estuar. Coast. Model. https://doi.org/10.1061/40628(268)19.

Thorne, P.D., Hanes, D.M., 2002. A review of acoustic measurement of small-scale sediment processes. Cont. Shelf Res. 22, 603–632.

Thorne, P.D., Hurther, D., Moate, B.D., 2011. Acoustic inversions for measuring boundary layer suspended sediment processes. J. Acoust. Soc. Am. 130, 1188–1200.

Tjensvoll, I., Kutti, T., Fosså, J.H., Bannister, R.J., 2013. Rapid respiratory responses of the deep-water sponge Geodia barretti exposed to suspended sediments. Aquat. Biol. 19, 65–73. https://doi.org/10.3354/ab00522.

Tompkins-MacDonald, G.J., Leys, S.P., 2008. Glass sponges arrest pumping in response to sediment: implications for the physiology of the hexactinellid conduction system. Mar. Biol. 154, 973–984. https://doi.org/10.1007/s00227-008-0987-y.

Trannum, H.C., Nilsson, H.C., Schaanning, M.T., Øxnevad, S., 2010. Effects of sedimentation from water-based drill cuttings and natural sediment on benthic macrofaunal community structure and ecosystem processes. J. Exp. Mar. Biol. Ecol. 383, 111–121. https://doi.org/10.1016/j.jembe.2009.12.004.

Vad, J., Kazanidis, G., Henry, L.A., Jones, D.O.B., Tendal, O.S., Christiansen, S., Henry, T. B., Roberts, J.M., 2018. Potential impacts of offshore oil and gas activities on Deep-Sea sponges and the habitats they form. Adv. Mar. Biol. 30 (79), 33–60. https://doi.org/10.1016/bs.amb.2018.01.001.

Vieira, R.P., Bett, B.J., Jones, D.O.B., Durden, J.M., Morris, K.J., Cunha, M.R., Trueman, C.N., Ruhl, H.A., 2020. Deep-sea sponge aggregations (Pheronema carpenteri) in the porcupine seabight (NE Atlantic) potentially degraded by demersal fishing. Prog. Oceanogr. 183 https://doi.org/10.1016/j.pocean.2019.102189.

Washburn, T.W., Turner, P.J., Durden, J.M., Jones, D.O.B., Weaver, P., Van Dover, C.L., 2019. Ecological risk assessment for deep-sea mining. Ocean Coast. Manag. 176, 24–39.

Wedding, L.M., Friedlander, A.M., Kittinger, J.N., Watling, L., Gaines, S.D., Bennett, M., Hardy, S.M., Smith, C.R., 2013. From principles to practice: a spatial approach to systematic conservation planning in the deep sea. Proc. R. Soc. Lond. B Biol. Sci. 280, 20131684 https://doi.org/10.1098/rspb.2013.1684.

Whalan, S., Battershill, C., de Nys, R., 2007. Variability in reproductive output across a water quality gradient for a tropical marine sponge. Mar. Biol. 153, 163–169.

Zhang, Y., Liu, Z., Zhao, Y., Wang, W., Li, J., Xu, J., 2014. Mesoscale eddies transport deep-sea sediments. Sci. Rep. 4, 1–7.